BMC Genomics

RESEARCH

Open Access

Transcriptomic analysis reveals genetic factors underlying impaired symbiotic nitrogen fixation in lines derived from crosses between cultivated peanut (*Arachis hypogaea* L.) and its wild ancestors

Darius Tchoutang Nzepang[1,2,3], Maïmouna Cissoko[2,3], Djamel Gully[3], Valérie Hocher[2,3], Jean-François Rami[4,5], Saliou Fall[2], Daniel Fonceka[4,5] and Sergio Svistoonoff[3*]

Abstract

Background Symbiotic nitrogen fixation (SNF) is a complex process regulated by numerous genes extensively studied in legumes that undergo intracellular infection, such as *Lotus japonicus*, *Medicago truncatula*, and *Glycine max*. However, the molecular and genetic mechanisms of SNF in legumes that rely on the intercellular infection pathway, such as peanut (*Arachis hypogaea* L.), remain poorly understood. In a previous study, we identified two chromosome segment substitution lines (CSSLs), 12CS_051 and 12CS_044, each contains a wild segment on homeologous regions of chromosomes A02 and B02 respectively, that are severely impaired in nitrogen fixation. In this study, we have compared the transcriptomes of those lines with that of their recurrent parent, Fleur11, in roots inoculated with the effective *Bradyrhizobium vignae* strain ISRA400 to identify candidate genes associated with the reduced nitrogen fixation observed in these CSSLs.

Results A comparative analysis of the transcriptome profiles of the CSSLs and Fleur11 revealed significant changes in the expression of genes involved in plant immune signaling and key symbiotic genes, such as *NIN*, *EFD, FEN1* or SNF-related transporters. These results align with the phenotypic differences observed during the symbiotic process in the CSSLs. When focusing on each QTL region, we found that only the orthologs of the symbiotic gene *FEN1*, which is responsible for the failure in the enlargement of infected cells in *L. japonicus*, exhibited a lack of expression in the two CSSLs compared to Fleur11. *FEN1* encodes a homocitrate synthase that is essential for the nitrogenase activity. We hypothesize that changes in the expression of *FEN1* could affect the nitrogenase activity, potentially leading to the unfair SNF observed in these lines.

Conclusions In this study, we analyzed the expression profiles of two ineffective nitrogen-fixing chromosome segment substitution lines and identified *FEN1* as a suitable candidate gene involved in peanut symbiosis. This research provides valuable insights into understanding and improving SNF in peanut.

Keywords Groundnut, Biological nitrogen fixation, Rhizobia, Molecular mechanisms, Quantitative genetics, Breeding

*Correspondence:
Sergio Svistoonoff
sergio.svistoonoff@ird.fr
Full list of author information is available at the end of the article

Background

Cultivated peanut (*Arachis hypogaea* L.) is an allotetraploid legume with an AABB genome ($2N = 4x = 40$), which originated from a single recent hybridization between two wild diploid species, *Arachis duranensis* ($2N = 2x = 20$, AA) and *Arachis ipaensis* ($2N = 2x = 20$, BB), followed by chromosome duplication [1]. Peanut is an important oilseed crop that can meet up to 55–68% of its nitrogen needs through symbiotic nitrogen fixation (SNF) [2, 3], thanks to its interaction with rhizobia of the genus *Bradyrhizobium* [4, 5]. The fixed nitrogen is vital for the growth and production of this legume crop, and also serves as an important nitrogen source for intercropped cereals especially in low input farming systems [6]. However, SNF in peanut is not yet well understood. In a previous study, we used a population of 83 chromosome segment substitution lines (CSSLs) derived from the cross between the cultivated peanut variety Fleur11 (AABB genome) and the synthetic tetraploid AiAd [(*A. ipaensis* Krapov. and W. C. Gregory, KG30076 (BB genome) ´ *A. duranensis* Krapov. and W. C. Gregory, V14167 (AA genome)]$^{4X´}$ [7], to identify quantitative trait loci (QTLs) related to nitrogen fixation. We identified four major QTLs, two of which were mapped on homeologous regions of chromosome A02 (line 12 CS_051) and chromosome B02 (line 12 CS_044) [8]. The wild alleles associated with these QTLs had a significant negative impact on several traits associated with nitrogen fixation such as chlorophyll content, plant biomass, nitrogenase activity and the presence of functional bacteroids [8]. The wild chromosome segments present in these two lines span approximately 76 Mbp on chromosome A02 and 82.5 Mbp on chromosome B02 and contain too many genes to pinpoint those that are likely responsible for the observed phenotypes.

In peanut, rhizobia penetrate the root through the middle lamella between adjacent root hair cells then spread intercellularly by separating cortical cells along their middle lamellae. Large basal cells associated with some axillary root hairs are the first cells to be infected intracellularly. These cells then undergo repeated divisions, ultimately forming nodule tissue [9]. However, the molecular and genetic mechanisms of SNF in legumes that rely on the intercellular infection pathway, remain poorly understood [10]. Over the past two decades, studies have focused on the genetic and molecular mechanisms of SNF in the model legumes *Lotus japonicus* and *Medicago truncatula*. In these species, rhizobial infection follows a distinct pathway, involving the formation of infection threads that enable intracellular bacterial entry through root hairs [11–13]. Briefly, the legume releases exudates containing flavonoids into the rhizosphere, which are recognized by soil rhizobia as symbiotic signals [14]. This recognition attracts the bacteria around the root by chemotaxis and leads to the production and release of Nod factors (NFs), which can be recognized by NF membrane receptors (*LjNFR1/LjNFR5* or *MtLYK3/MtNFP*) on plant cells [12]. NF recognition leads to nuclear calcium oscillations caused by the activation of an NF co-receptor (*LjSYMRK*/*MtDMI2*), membrane proteins (*LjCASTOR*, *LjPOLLUX*/*MtDMI1*) and nucleoproteins (*LjNUP85*, *LjNUP133*, *LjNENA*) [11]. Subsequently, a complex consisting of the proteins *LjCCamK*/*MtDMI3* and *LjCYCLOPS*/*MtIPD3* decodes these calcium oscillations and induces several transcription factors (TF) such as *LjNSP1*, *LjNSP2*, *LjNIN*, *LjCRE1*, *LjERN1*, which are key genes involved in bacterial infection and nodule organogenesis [11, 12]. Afterwards, nodule functioning requires genes involved in the activation of the bacterial nitrogenase, metabolism and transport, such as leghemoglobins (*LjHB*), nitrogenase dependent cofactor homocitrate (*FEN1*), symbiotic ammonium transporter (*GmbHLm1*), copper transporter (*MtCOP1*) and iron transporter (*LjSEN1*) [13].

RNA-Seq has widely been used in some model legumes crops such as soybean and common bean to gain insights into global gene expression and the molecular mechanisms involved in SNF [15–20]. The recent genome sequencing of cultivated peanut and its two wild diploid ancestors (*A. duranensis* and *A. ipaensis*) [1, 21, 22], offers the opportunity to start deciphering the genetic and molecular basis of the SNF process. For example, phylogenetic and transcriptomic analysis allowed, on the one hand, to identify the orthologs of many symbiotic genes previously described in model legumes and, on the other hand, to study their expression profiles during the SNF process [13, 23–28]. In addition, functional analyses available for a small set of symbiotic genes like *AhCCaMK*, *AhCYCLOPS*, *AhHK1*, *AhNFR1*, *AhNFR5*, and *AhNSP2* confirmed that the main molecular actors involved in the nodulation of model legumes play a similar role in peanut [29–33]. However, certain genes like *RPG* (Rhizobium Directed Polar Growth) required for infection thread formation during intracellular infection are absent in peanut [9, 23, 25–28], pointing out the existence of different molecular mechanisms that thus, that have not yet been explored.

In this study, we performed a comparative analysis of the transcriptome profiles of the two CSSLs and their recurrent parent Fleur11, to identify transcriptional signatures and candidate gene (s) related to the Fix- phenotypes observed in these CSSLs. Specific and differential expression patterns of genes were identified between the CSSLs and Fleur11. We identified *FEN1* as a potential candidate gene located in the wild chromosome segments carried by the two CSSLs. These findings provide a

basis for further investigations to elucidate the molecular mechanisms underlying nitrogen fixation in peanut.

Materials and methods

Plant materials and experimental design

Two CSSLs (12 CS_051 and 12 CS_044) along with their recurrent parent Fleur11 were descripted in our previous study [7]. The two CSSLs exhibited a lower symbiotic efficiency compared to Fleur11 when inoculated with *Bradyrhizobium vignae* strain ISRA400 [8]. For each genotype, the seeds were provided by the Centre de Recherche pour l'Amélioration de l'Adadptation à la Sécheresse (CERAAS) located in Thiès, Senegal, which developed the CSSL population. The rhizobial strain ISRA400 was provided by the Laboratoire Commun de Microbiologie (LCM) located in Dakar, Senegal, which maintains a large collection of peanut rhizobia.

The seeds were sterilized using a 7% calcium hypochlorite solution, then washed three times with sterilized water. They were germinated on water agar Petri dishes medium for three days at 28 °C [5]. Afterward, the seedlings were transplanted into Leonard jars filled with sterilized vermiculite [34] and watered with nitrogen-free BNM nutrient solution [35]. Two treatments were applied: one without nitrogen, and another without nitrogen but inoculated with the efficient *B. vignae* strain ISRA400 [5]. Three time points were investigated: 0, 12 and 21 days post-inoculation (dpi). The experimental design was a randomized complete block with five replicates. For each genotype, one replicate corresponds to one plant. The plants were grown in a growth chamber at 28 °C with a photoperiod lighting 16 h of light (150 mmol. $m^2.s^{-1}$) and 8 h of darkness and 70% humidity. Seven days after planting, each seedling was inoculated with 1 ml of *B. vignae* inoculum. The inoculum was prepared by culturing the bacteria in yeast mannitol medium in the dark for 4 days at 28 °C while shaking at 250 rpm, until a cell suspension with an absorbance of approximately 0.7 at 600 nm. Non-inoculated plants served as control group. Nitrogen fixation effectiveness was assessed 21 days after inoculation (dpi) by estimating the leaf chlorophyll content of the third youngest leaf using a SPAD meter (soil plant analysis development; Konica-Minolta, Okasaka, Japan) [8]. Each CSSL was compared to the recurrent parent Fleur11 with Dunnett's multiple test at $p < 0.05$ using R software [36], as described in [8]. For each genotype, the whole root system of three replicates was harvested at 0, 12, and 21 dpi, and the collected samples were cleaned and immediately frozen in liquid nitrogen for RNA extraction. The remaining two replicates were used for histological analyses of nodules. The harvested time points 12 and 21 dpi, were selected according to previous results [26, 27], and correspond to immature and mature nodule development stages in peanut.

Histological analyses of nodules

For each genotype, nodule development was recorded at 0, 12 and 21 dpi. Macroscopic observations of nodules and roots were conducted using a SMZ74557 stereoscopic microscope (Nikon, Tokyo, Japan) equipped with a GO-3 camera (Q-Imaging, Ontatio, Canada). Images were captured using Q-capture software (Q-Imaging). To visualize the structure of nodules and their infection by the bacteria, fresh nodules were excised at 21 dpi, fixed in 4% paraformaldehyde for 24 h at 4 °C, and then stored at room temperature in 70% ethanol. Four to five nodules were dehydrated in an ethanol gradient (80, 90, 95, and 100%) and embedded in a Technovit 7100 resin (Kulzer, Hanau Germany). The embedded samples were sectioned at 5–6 µm using an RM 2145 rotary microtome (Leica Biosystems, Nussloch, Germany). Finally, the sections were stained with 0.01% toluidine blue for 2 min and observed using a H550S light microscope (Nikon, Tokyo, Japan) equipped with a Micropublisher 3.3 STV camera (Q-Imaging, Ontario, Canada).

RNA extraction, cDNA library construction and sequencing

Frozen samples were individually ground into a fine powder in liquid nitrogen using a mortar and a pestle. For each sample, the total RNA was extracted from approximately 100 mg of powdered material by following the RNeasy Minikit protocol (Qiagen, Hilden, Germany). cDNA libraries were constructed using Stranded mRNA Prep ligation kit (Illumina, San Diego, USA) and 2 µg of total RNA. In total, 27 libraries (3 genotypes ´ 3 stages ´ 3 replicates) were generated and sequenced on a NovaSeq 6000 sequencer (Illumina, San Diego, USA) at MGX-Montpellier Genomix platform (MGX, France, https://www.mgx.cnrs.fr/index.php). Libraries were sequenced in single reads of 100 nucleotides.

Quality control and sequence data preprocessing

The quality of the raw reads from the RNA-seq was analyzed using Fastqc (https://www.bioinformatics.babraham.ac.uk/projects/). Adapters and low-quality sequences (Phred score < 30) were removed using Cutadapt [37]. The remaining high-quality sequences were aligned to the *A. hypogaea* var. Tifrunner reference genome (arahy.Tifrunner.gnm1.KYV3.genome_main.fna, downloaded from PeanutBase: https://www.peanutbase.org/) using the nf-core/rnaseq pipeline [38, 39]. Briefly, reads were aligned to the reference sequence using STAR [40]. The quality of the alignment was assessed using Qualimap [41], and gene expression was quantified using Salmon [42] to count the reads that mapped to a single

gene model annotated in the *A. hypogaea* var. Tifrunner GFF file (arahy.Tifrunner.gnm1.ann1.CCJH.gene_models_main.gff3, downloaded from PeanutBase.

Identification of differentially expressed genes, gene ontology enrichment

For each genotype, the expression levels of transcripts from control samples (0 dpi) and inoculated (12, 21 dpi) samples were compared to identify differentially expressed genes (DEGs) during the SNF process. The DEGs were identified using the EdgeR Bioconductor package [43]. Only genes with a False Discovery Rate, adjusted by the Benjamini & Hochberg method, of ≤ 0.05 and an absolute log2 FoldChange (log2 FC) of ≥ 2 were considered differentially expressed. Veen diagrams, heat maps, and volcano plots were generated using the ggveen [44], ComplexHeatmap [45] ggplot2 [46] packages respectively. The Gene Ontology (GO) terms for DEGs in the genome annotation were also retrieved from the GFF file downloaded from PeanutBase website. To investigate the cellular components (CC), molecular functions and biological process (BP) associated with DEGs, GO term enrichment analysis was performed using Goseq Bioconductor package (Galaxy version 1.50.0 +galaxy0), based on the Wallenius method [47]. For the annotated GFF file, we classified and plotted DEGs according to the official classification using Wego 2.0 [48, 49].

Identification of symbiotic genes

We identified orthologs of genes known to be involved in root nodule symbiosis in other species using the Orthofinder pipeline [25, 50]. The database comprised the proteomes of 14 legumes: *A. hypogaea*, *A. ipaensis*, *A. duranensis*, *Cercis canadensis*, *Phaseolus vulgaris*, *Vigna unguiculata*, *Glycine max*, *L. japonicus*, *M. truncatula*, *Lupinus albus*, *Aeschynomene evenia*, *Nissolia schottii*, *Chamaecrista fasciculata* and *Mimosa pudica*. These were downloaded from the Legume Information System (https://legumeinfo.org/https://legumeinfo.org/) and the National Center for Biotechnology (https://www.ncbi.nlm.nih.govhttps://www.ncbi.nlm.nih.gov) websites. The analysis led to the identification of 228 orthogroups containing 248 symbiotic genes [13, 51, 52] and 856 peanut orthologs potentially involved in SNF. Those genes are hereinafter referred as orthologs of symbiotic genes. The expression profile of these peanut orthologs was analyzed in each genotype. Steps used to identify orthologs of symbiotic genes in each QTL region that are differentially expressed are summarized in Supplementary Data (Fig. S1).

Quantitative reverse transcription PCR (qRT-PCR) analysis

qRT-PCR were performed using the same samples previously used for RNAseq experiments. However, the Fleur11 replicate sample at 12 dpi that appeared to be outlier (see results) was replaced with another sample corresponding to the same conditions. Single strand cDNA was synthesized from 500 ng of total RNA using Quanti Tect Reverse Transcriptase kit (Qiagen, Hilden, Germany). qRT-PCR was performed on a StepOne Applied Biosystems apparatus (Thermo Fisher Scientific, Waltham, MA, USA) with the Takyon SYBR qPCR Blue Master Mix (Eurogentec, Seraing, CA, Belgium) under the following conditions: 95 °C for 5 min, 40 cycles of 95 °C for 10 s, and 60 °C for 30 s. The primer set was designed using Beacon Designer software (Premier Biosoft International, Palo Alto, CA, USA) and can be seen as Supporting Information (Table S1). Expression values were normalized using the expression level of the *AhUBC1* gene encoding ubiquitin.

Results

The two CCSLs exhibit symptoms associated with nitrogen fixation impairment

Traits related to nitrogen fixation were assessed between the two CSSLs and Fleur11 at 21 dpi. In the control treatment, no difference in leaf chlorophyll content (measured by SPAD) was observed between the genotypes. However, in the inoculated treatment, the CSSLs displayed significantly lower leaf chlorophyll content compared to Fleur11 indicating that nitrogen fixation was impaired in those CSSLs as previously described [8] (Fig. S2). Prior to inoculation, no nodules were detected in the roots for all genotypes (Fig. 1a, f, k). Fleur11 formed immature nodules (white color) at 12 dpi (developmental stage) which evolved to mature nodules (pink color) at 21 dpi (functional stage) (Fig. 1b and c). The histological analysis of nodule sections from

(See figure on next page.)

Fig. 1 Nodule development and histological features in plants inoculated with a *Bradyrhizobium vignae*. Fleur11, the recurrent parent and the two segment substitution lines 12 CS_051 and 12 CS_044 are shown per column from left to right. **a**-**c**, **f**–**h** and **k**-**m**: micrographs of root systems at 0, 12 and 21 days post inoculation (dpi) (scale bar = 500 µm). **d**, **i** and **n**: longitudinal sections of nodules at 21 dpi stained with toluidine blue (d-n: scale bar = 100 µm). **e**, **j** and **o**: magnified areas of **d**, **i** and **n** sections, showing infected plant cells (scale bar = 10 µm). * Corresponds to the areas of **d**, **i** and **n** magnified in **e**, **j** and **o**. FZ = fixation zone, VB = vascular bundles, NP = nodule parenchyma, *N* = nucleus, DB = differentiated bacteria, UB = undifferentiated bacteria, V = vacuole

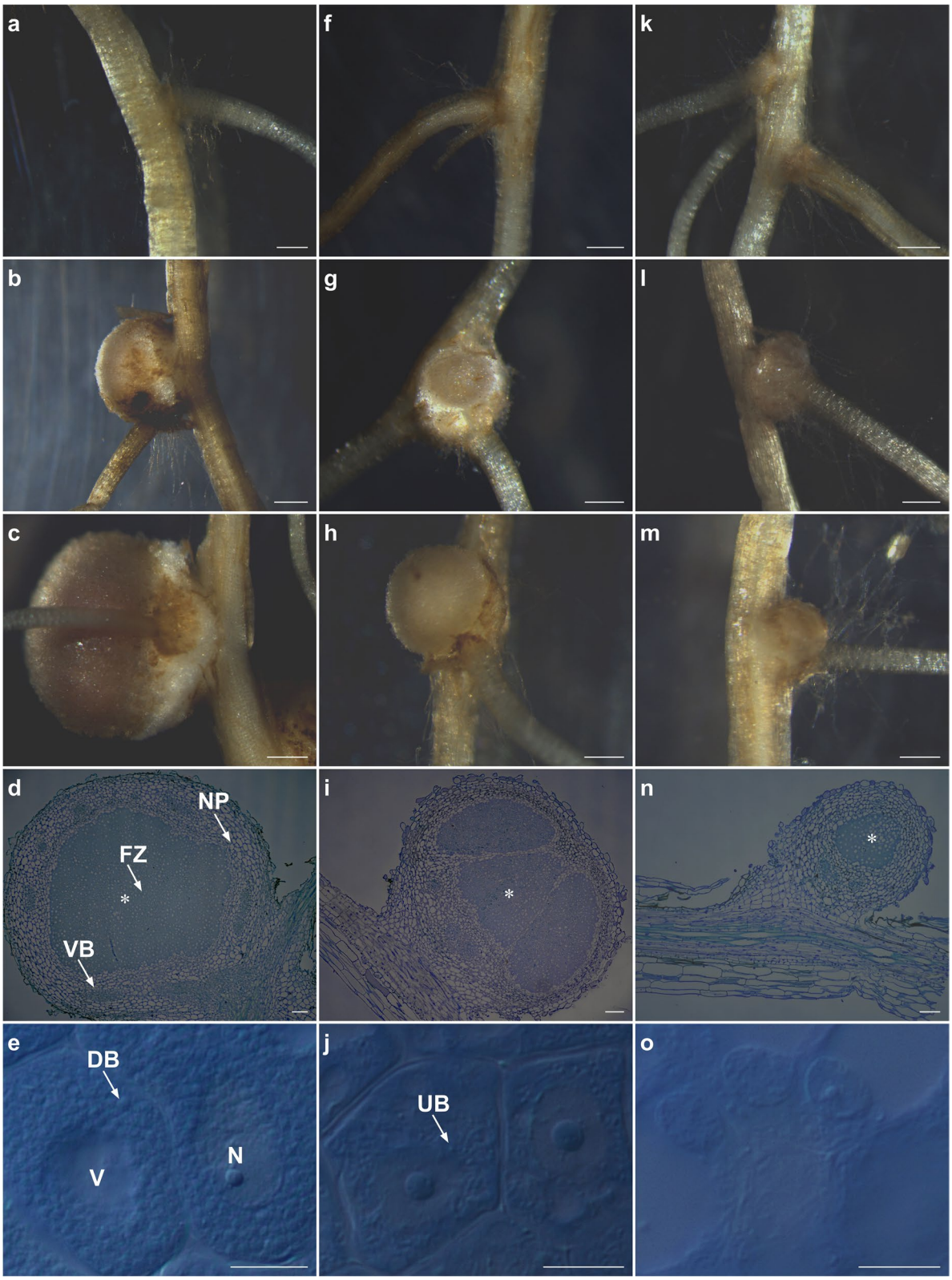

Fig. 1 (See legend on previous page.)

Fleur11 at 21 dpi showed an aeschynomenoid-type tissue structure. This includes a central area (fixation zone) infected by bacteria, which terminally differentiated into bacteroids with the characteristic rounded shape, a peripheral parenchyma composed of uninfected cells, and vascular bundles (Fig. 1d and e). Both CSSLs displayed a nodule structure similar to that of Fleur11 at 21 dpi except that the nodules formed by line 12 CS_051 were slightly smaller and appeared immature (Fig. 1g and h). Histological sections indicated that very few bacteria in this line had differentiated into bacteroids (Fig. 1i and j). For line 12 CS_044, we observed immature nodules of very small size, characterized by a scarce number of infected cells and the presence of a few bacteroids in the intracellular space (Fig. 1l-o). A similar number of nodules was observed in 12 CS_051 compared to Fleur11, but slightly fewer nodules were present in line 12 CS_044 (data not shown).

Sequencing, quality analyses, and mapping

A total of approximately 1.2 Gb of clean reads was obtained from the 27 RNA-seq libraries, averaging ~ 44 Mb per sample. The data size per sample and stage ranged from 36 to 62 Mb on average (Table 1). All samples showed standard %GC contents (43–46%), indicating the RNA sequencing reads were of good quality. In total, 52% to 66% of the reads were uniquely mapped to the *A. hypogaea* genome, with an average of 35% of the reads mapped to more than one locus (Table 1). Out of the 67,124 genes annotated in the *A. hypogaea* cv. Tifrunner genome (from PeanutBase), 61.9% passed the post-quality filtering criteria, resulting in a final set of 41,559 genes for further analysis. A principal component analysis revealed a clear distinction between the uninoculated (0 dpi, or control) group and the inoculated groups (12 and 21 dpi). Good reproducibility was observed between biological replicates, except for one Fleur11 sample at 12 dpi (Fig.

Table 1 Summary of raw Illumina sequencing reads after preprocessing and mapping to *A. hypogaea* genome in each library

RNA extraction stage	Samples	Clean reads	Mapped reads (%)	Uniquely mapped (%)	Multiple loci mapped (%)	%GC
0 dpi	Fleur11-R1	48,496,083	98.9	63.6	35.3	44
	Fleur11-R2	55,297,710	98.8	63.3	35.5	44
	Fleur11-R3	39,751,820	98.7	63.2	35.5	44
	12 CS_051-R1	46,866,066	98.8	62.8	36	44
	12 CS_051-R2	54,597,493	98.8	62.9	35.9	44
	12 CS_051-R3	42,689,417	98.5	62.5	36	44
	12 CS_044-R1	42,187,774	98.5	62.7	35.8	43
	12 CS_044-R2	51,378,233	98.5	62.5	36	44
	12 CS_044-R3	47,997,547	98.4	62.9	35.5	44
12 dpi	Fleur11-R1	46,333,603	83	52.6	30.4	46
	Fleur11-R2	54,100,316	97	61.3	35.7	44
	Fleur11-R3	86,165,092	98.3	62.2	36.1	45
	12 CS_051-R1	44,167,388	97.6	61.6	36	44
	12 CS_051-R2	25,994,541	98.2	62.2	36	44
	12 CS_051-R3	38,373,385	97.3	61.2	36.1	45
	12 CS_044-R1	38,808,175	97.7	60.7	37	45
	12 CS_044-R2	44,513,728	96.6	60.5	36.1	45
	12 CS_044-R3	44,487,845	97.6	61.2	36.4	45
21 dpi	Fleur11-R1	38,299,519	99	65.7	33.3	43
	Fleur11-R2	44,037,899	99	65.4	33.6	44
	Fleur11-R3	37,543,103	99.2	66	33.2	43
	12 CS_051-R1	43,058,388	98	63.2	34.8	44
	12 CS_051-R2	44,187,512	99	63.8	35.2	44
	12 CS_051-R3	35,315,475	98.8	64.2	34.6	43
	12 CS_044-R1	33,690,447	98.6	63.2	35.4	44
	12 CS_044-R2	38,098,437	99	63.3	35.7	44
	12 CS_044-R3	39,080,945	98.9	63.5	35.4	44

dpi means days post-inoculation. R1, R2 and R3 correspond to the replicates sequenced for genotype at each stage

S3a). For further analysis, this particular sample was considered as an outlier and removed (Fig. S3b). The results obtained for this developmental stage are provided in the Supplementary Data (Fig. S9, Table S2, S3 and S6).

Identification of differentially expressed genes

At the functional stage, a total of 4243, 2383, and 2549 DEGs were identified in Fleur11, 12 CS_051, and 12 CS_044, respectively (Fig. 2a). In Fleur11, most of the downregulated (55–63%) and upregulated (43–52%) genes were not shared with either of the two CSSLs (Fig. 2b and c). This distribution of DEGs likely indicates strong differences in gene expression between the

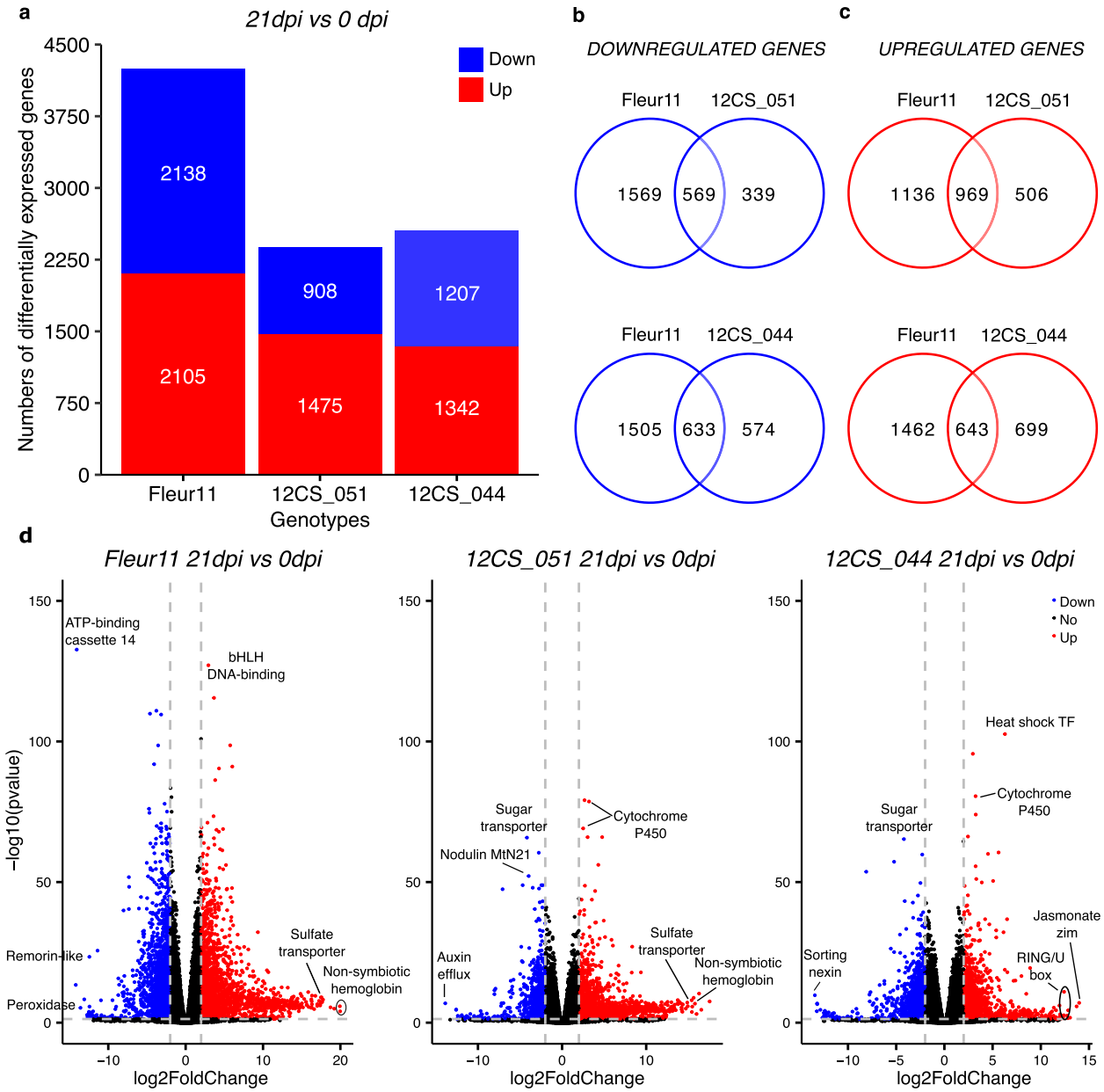

Fig. 2 Gene expression profile in the recurrent parent Fleur11 and the CSSLs 12 CS_051 and 12 CS_044 between 0 and 21 days post-inoculation. **a** Bar plot of the number of differentially expressed genes (DEGs) identified of each genotype. **b**, **c** Venn diagrams showing the number of DEGs downregulated and upregulated in Fleur11 and each CSSL. **d** Volcano plots of gene expression showing the significance level (p-value ≤ 0.05) of gene expression (log2 FoldChange ≤ −2 or ≥ 2) for each genotype

functional nodules of Fleur11 and the poorly functional nodules of the two CSSLs. A Volcano plot illustrating for each genotype, the significance of differences in gene expression between control and inoculated samples is presented in Fig. 2d.

Functional classification of DEGs

To investigate the functional categories associated with differential gene expression between Fleur11 and the two CSSLs we performed a gene ontology (GO) analysis.

Transcriptome profile description of Fleur11

In Fleur11, GO term enrichment analysis of 4243 DEGs, including 2138 downregulated and 2105 upregulated genes, identified 63 significantly enriched GO terms, distributed across 21 biological process (BP), 30 molecular functions (MF), and 11 cellular components (CC) (Table S2). Gene functions related to responses to biotic stimulus, oxidative stress and bacteria, and DNA transcription were particularly over-represented (Table S2). Among the most highly expressed genes were those encoding non-symbiotic hemoglobin (*Arahy.C5DNVC, Arahy.9R3RK8*, *Arahy.SU9 WSI*), sulfate transporter (*Arahy.0G5 TBZ, Arahy.WH3 JRW*), subtilisin-like serin protease (*Arahy.8L903M*, *Arahy.4RTA8 J*), and *cysteine-rich secretory proteins, antigen 5, and pathogenesis-related 1 proteins* (*CAPs*) (*Arahy.USL2 FX, Arahy. HUGM4D*) and several genes encoding uncharacterized proteins (Fig. 2d, Table S3).

Comparison of transcriptome profiles between line 12 CS_051 and Fleur11

A GO term enrichment was conducted on the 339 downregulated and 506 upregulated genes that were exclusively detected in line 12 CS_051 when compared to Fleur11 (Fig. 2b and c). A total of ten GO terms related to oxidoreduction activity, cell wall and enzyme inhibitor activity were significantly enriched among the downregulated genes (Fig. 3a, Table S4). For upregulated genes, 10 GO terms were significantly enriched, including “heme binding” and “protein serine/threonine kinase activity” (Fig. 3b, Table S4). In addition, we performed a functional classification on 1569 downregulated and 1136 upregulated genes in Fleur11 which displayed expression levels that were not changed in line 12 CS_051 (Fig. 2b and c). The functional classification of the downregulated genes revealed 28 significantly enriched GO terms, such as “response to biotic stimulus”, “heme binding”, “O-glycosyl hydrolase activity” and “response to oxidative stress” (Fig. 3c, Table S4). For the upregulated genes, six GO terms were significantly enriched, including “DNA transcription” and “oxidoreduction activity” (Fig. 3d, Table S4). The most highly expressed genes in line 12 CS_051, as in Fleur11, include genes encoding a non-symbiotic hemoglobin, a sulfate transporter, and a subtilisin-like serin protease (Fig. 2d, Table S3).

Comparison of transcriptome profiles between line 12 CS_044 and Fleur11

A total of 574 downregulated and 699 upregulated genes were identified exclusively in line 12 CS_044 when compared to Fleur11 (Fig. 2b and c). Among the downregulated genes, 19 Go terms including"response to biotic stimulus","cell wall", and"oxidoreduction activity"(Fig. 4a, Table S4) were significantly enriched. For the 699 upregulated genes, 18 GO terms were overrepresented, including functions such as"defense response","heme binding", and"protein kinase activity"(Fig. 4b, Table S4). In contrast, in Fleur11, we identified 1505 downregulated and 1462 upregulated genes, that did not show significant expression in line 12 CS_044 (Fig. 2b and c). The functional classification of the downregulated genes revealed 22 GO terms significantly enriched, encompassing"response to biotic stimulus","response to oxidative stress","heme binding", and"O-glycosyl hydrolase activity"(Fig. 4c, Table S4). Among the upregulated genes, 11 GO terms were significantly enriched, relating functions such as"DNA transcription","b-glucanases activity", and"oxidoreduction activity"(Fig. 4d, Table S4). In contrast to Fleur11, genes associated with the jasmonic acid pathway, such as those encoding jasmonate-zim-domain protein 1 (*Arahy.DQCW8 K*) and RING/U-box protein (*Arahy.UIUY7Y/Arahy.N0BVKE*) were found among the most highly expressed genes in line 12 CS_044, (Fig. 2d, Table S3). Nevertheless, some orthologs of genes encoding a non-symbiotic hemoglobin and a sulfate transporter were also highly expressed in line 12 CS_044 (Table S3).

Identification and analysis of expression of symbiotic genes

In order to identify the DEGs that are likely to be directly involved in SNF, we performed an Orthofinder analysis to identify the peanut orthologs of genes that were shown to be involved in SNF in other legumes.

Identification of orthologs of known symbiotic genes in the peanut genome

Based on the available proteomes from several legumes including those from the two models, *M. truncatula* and *L. japonicus*, the Orthofinder analysis allowed the identification of peanut orthologs of 212 symbiotic genes described in other species (Table S5) [13, 25, 27, 52]. Notably, we did not find orthologs for a subset of 36 known symbiotic genes. This subset includes genes that are absent from the peanut genome such as *RPG*, *LegH* (Leghemoglobin), *DNF*2/7 (Defective in Nitrogen

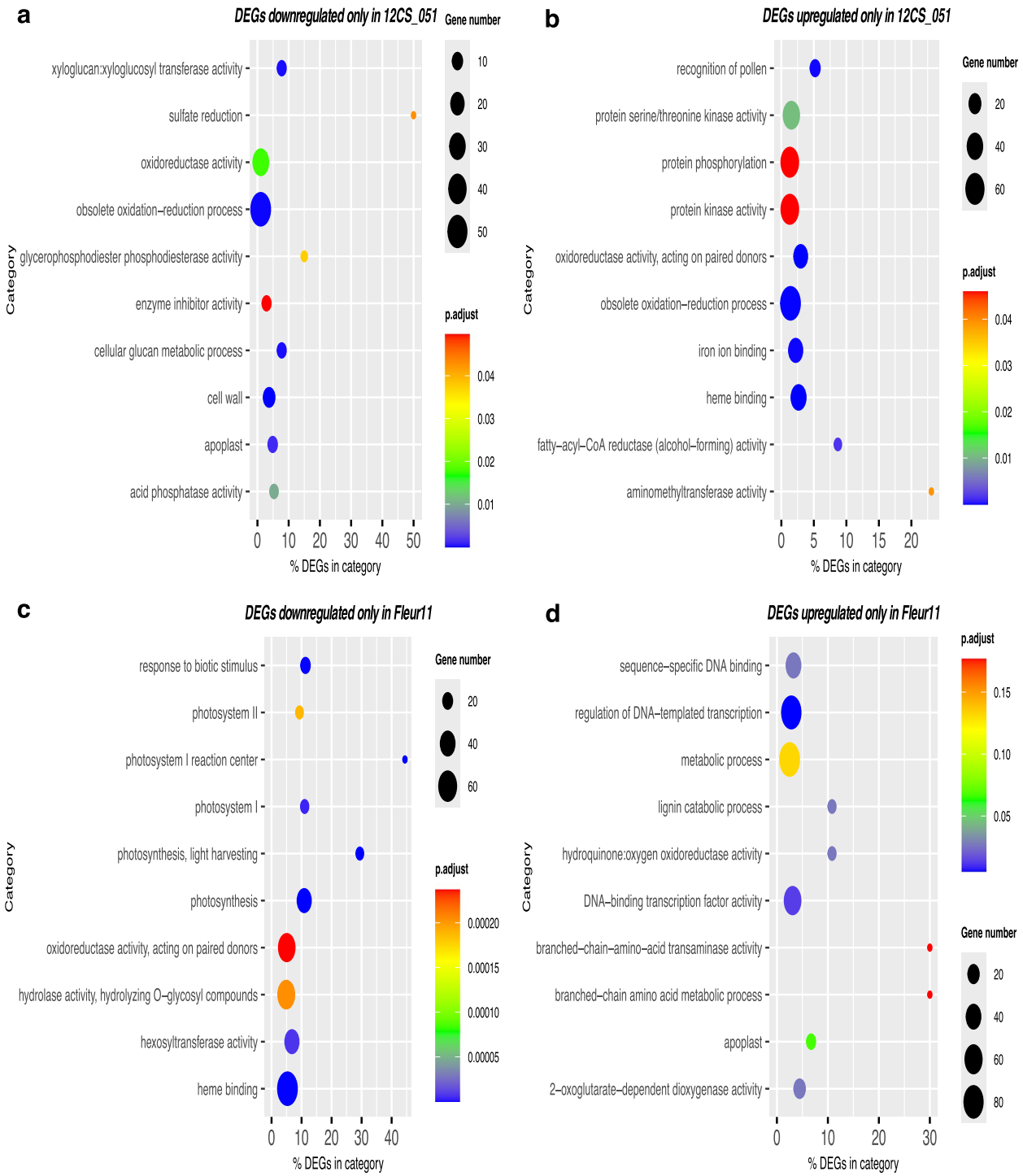

Fig. 3 Top 10 significantly enriched GO terms of differentially expressed genes identified only in Fleur11 or line 12 CS_051. The p.adjust is the corrected *p*-value ranging 0 to 1. **a**, **b** and **c**, **d** correspond to GO terms significantly enriched in downregulated and upregulated genes exclusively in line 12 CS_051 and Fleur11, respectively

Fixation), *CLE12* (Cytokinin signaling) or *SymCRK* (Symbiotic Cysteine-rich Receptor-like Kinase) as previously described by [27]. Among this subset of genes, certain are not yet annotated in the peanut genome and are absents in the peanut proteome, but their presence can be confirmed by BLAST analysis, such as *NSP2* (Nodulation

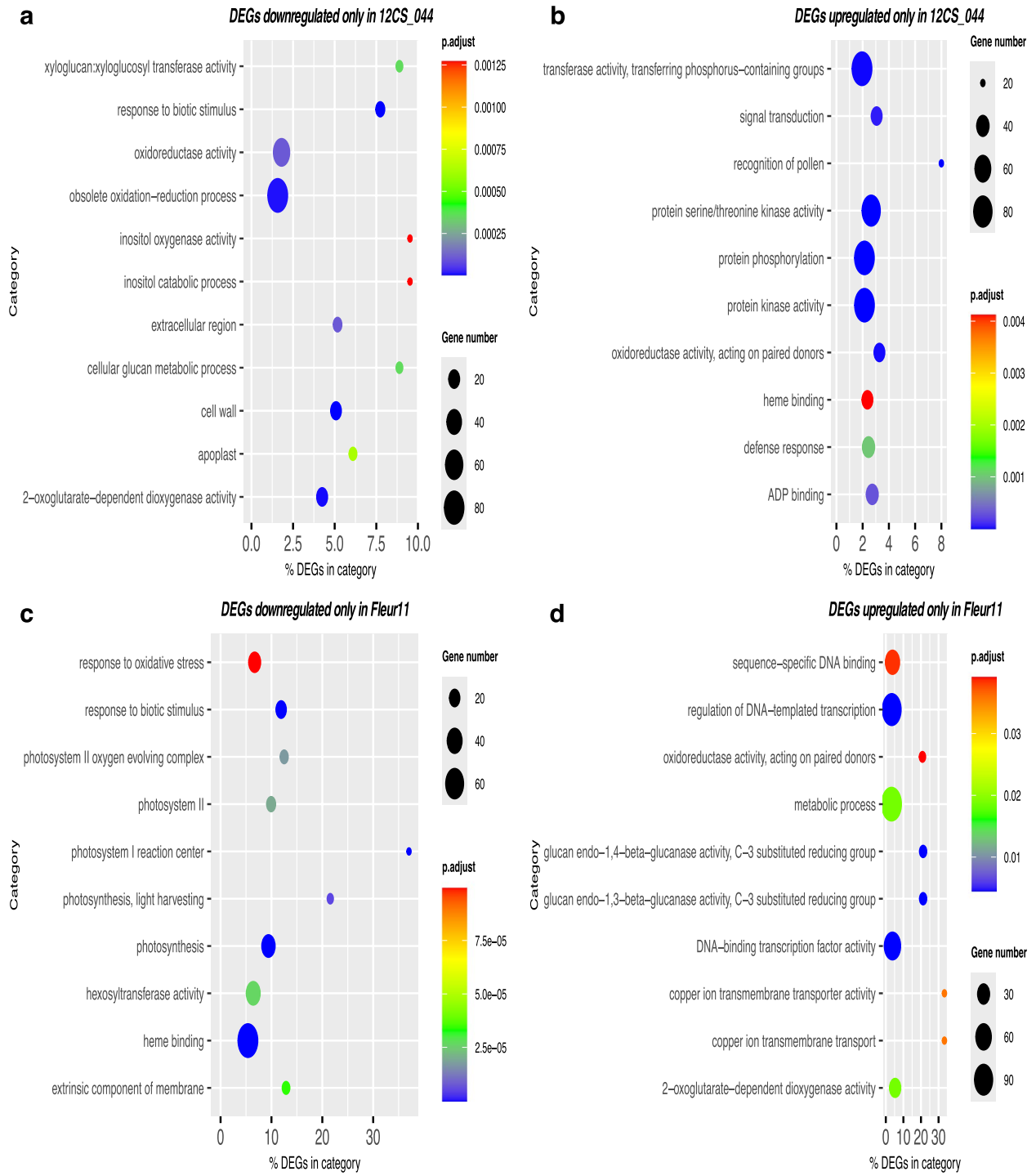

Fig. 4 Top 10 significantly enriched GO terms of differentially expressed genes identified only in Fleur11 or line 12 CS_044. The p.adjust is the corrected *p*-value ranging 0 to 1. **a**, **b** and **c**, **d** correspond to GO terms significantly enriched in downregulated and upregulated genes exclusively in line 12 CS_044 and Fleur11, respectively

Signaling Pathway), *ERN1/2* (Ethylene response factor required for nodulation), *LAN* (Lack of Symbiont Accommodation), *CLV2* (CLAVATA2, receptor-like protein), *CLE13* or *RSD* (Regulator of symbiosome development). The orthologs of symbiotic genes clearly identified in peanut genome were categorized into seven different functions based on their role during the nodulation process, as described by Raul et al. [27] and Roy et al. [13].

Peanut orthologs of symbiotic genes show different patterns in CSSLs compared to Fleur11

A total of 116, 82 and 77 orthologs of symbiotic genes were among the DEGs in Fleur11, line 12 CS_051 and line 12 CS_044, respectively (Table S6). Interestingly, we found several orthologs of symbiotic genes among the genes showing the highest expression levels in Fleur11 (Table S3). These included *Glb1/AhSymH1-3* (*Arahy.C5DNVC, Arahy.9R3RK8* and *Arahy.SU9 WSI*), encoding class I hemoglobins (phytoglobins also called non-symbiotic hemoglobin) that have replaced leghemoglobins in peanut, *SST1* (*Arahy.0G5 TBZ/Arahy.WH3 JRW*) encoding a sulfate transporter, and *AglAG12* (*Arahy.4RTA8 J*), encoding a subtilase (Tables S3 and S6). Furthermore, RNA-Seq analysis revealed that two orthologs of the Nodule Inception (*NIN*) gene, *Arahy.I65 W25*/*Arahy.V4BGUX,* which serves as a master symbiotic regulator of various genes and process related to nodule organogenesis, were significantly induced (Table S6). In 12 CS_051, the orthologs of *SST1*, *SymH*, and *AglAG12* were also among the highly expressed genes, and *NIN* gene orthologs were induced, though at lower levels compared to Fleur11 (Tables S3 and S6). In contrast, only two phytoglobin orthologs were among the highly expressed genes in the line 12 CS_044, and remarkably, none of the *NIN* orthologs was induced (Tables S3 and S6).

A comparative analysis of the differentially expressed orthologs of symbiotic genes in Fleur11 and the CSSLs revealed significant expression differences in genes involved in various symbiotic functions (Fig. S4). For instance, several orthologs of SNF genes involved in bacterial recognition and early signaling were induced only in the CSSLs compared to Fleur11. These included genes coding for a nucleotide binding site leucine-rich repeat resistance protein (*Rj2*), a chalcone synthase (*CHS*) and a chalcone reductase (*CHR*) (Fig. S4). On the other hand, some orthologs of key genes required for nodule organogenesis such as response regulator (*RR5/9/11*), ethylene response factor (*EFD*), nodule root transcriptional regulator (*NOOT*) and KNOX homeodomain (*KNAT3/5/9/10*), were not induced in the CSSLs (Fig. S4), pinpointing the reduction of nodule size observed in these CSSLs.

Focusing on 33 known symbiotic genes required for nodule functioning (symbiosome formation, and nodule metabolism and transport) at 21 dpi, which corresponds to a mature nodule stage, we observed upregulation of several genes encoding SNF-related transporters in Fleur11. These included copper transporter (*COP1*), symbiotic ammonium transporter (*GmbHLm1*), sulfate transporter (*SST1*), zinc efflux transporter (*MTP2*), molybdate transporter (*MOT1.2*), oxygen carrier hemoprotein (*Glb1/Glb3-2*) (Fig. 5). In contrast, orthologs of genes encoding the iron transporter (*NRAMP*), water channels (*TIP1 g*) and ammonium transporter (*AMT.1.1*) were downregulated. Additionally, orthologs of *FEN1* (a homocitrate synthase involved nitrogenase activity) and *SymREM1* (remorin protein involved in symbiosome formation) were induced in Fleur11. When comparing 12 CS_051 with Fleur11, a similar gene expression pattern was observed, except for two orthologs of *MTP2* and *Glb3-2,* and one of *MOT1.2* and *FEN1*, which exhibited significantly lower expression levels in line 12 CS_051(Fig. 5). In line 12 CS_044, however, most of genes encoding SNF-related transporters were not significantly induced compared to Fleur11. These include three orthologs of *Glb3-2* and *COPT1*, two orthologs *MTP2* and *GmbHLm1*, and one ortholog of *MOT1.2*. Furthermore, two orthologs of *FEN1*, exhibited a significant lower level of expression in line 12 CS_044 (Fig. 5).

In addition to the orthologs of 212 symbiotic genes identified in the peanut genome, we also investigated the expression of genes encoding a cysteine-rich proteins and peptides, which are associated with plant-pathogen interaction and terminal differentiation of rhizobia. In Fleur11, we observed a significant induction of 22 genes encoding *defensin-like nodule specific cysteine-rich peptides* (*NCRs*), and 43 *CAPs*, 40 of which are known to be specially induced in nodules (Table S7, Fig. S5). Some *NCRs* and *CAPs* genes were also induced in the CSSLs, although at lower levels compared to Fleur11, especially in line 12 CS_044 (Fig.S5).

qRT-PCR analysis performed on a set of seven genes, including *NIN, FEN1*, and *AglAG12*. In each genotype, the expression patterns of at least six genes were consistent with the RNA-Seq data across the different stages of the SNF process in each genotype (Table 2). The results of qRT-PCR strongly corroborated the finding from RNA-seq analysis.

Analysis of gene expression in regions corresponding to the QTLs

To investigate the candidate gene(s) responsible for the impaired symbiotic phenotypes recorded in the two CSSLs, we focused our analysis on genes located in the QTL regions on chromosomes A02 (line 12 CS_051) and B02 (12 CS_044). The targeted regions are located between SSR markers Seq12E03 and RM2H10 on chromosome A02, and between the SSR markers Seq1B09 and Ah3 TC13E05 on chromosome B02 [8]. The QTL on chromosome A02 is 76 Mbp in size and contains 1180 annotated genes. On chromosome B02, the QTL is 82.5 Mbp in size and contains 1095 annotated genes. The comparison of QTL sequences from homeologous chromosomes A02 and B02 of *Arachis hypogaea* cv. Tifrunner revealed a good collinearity suggesting that the sequences

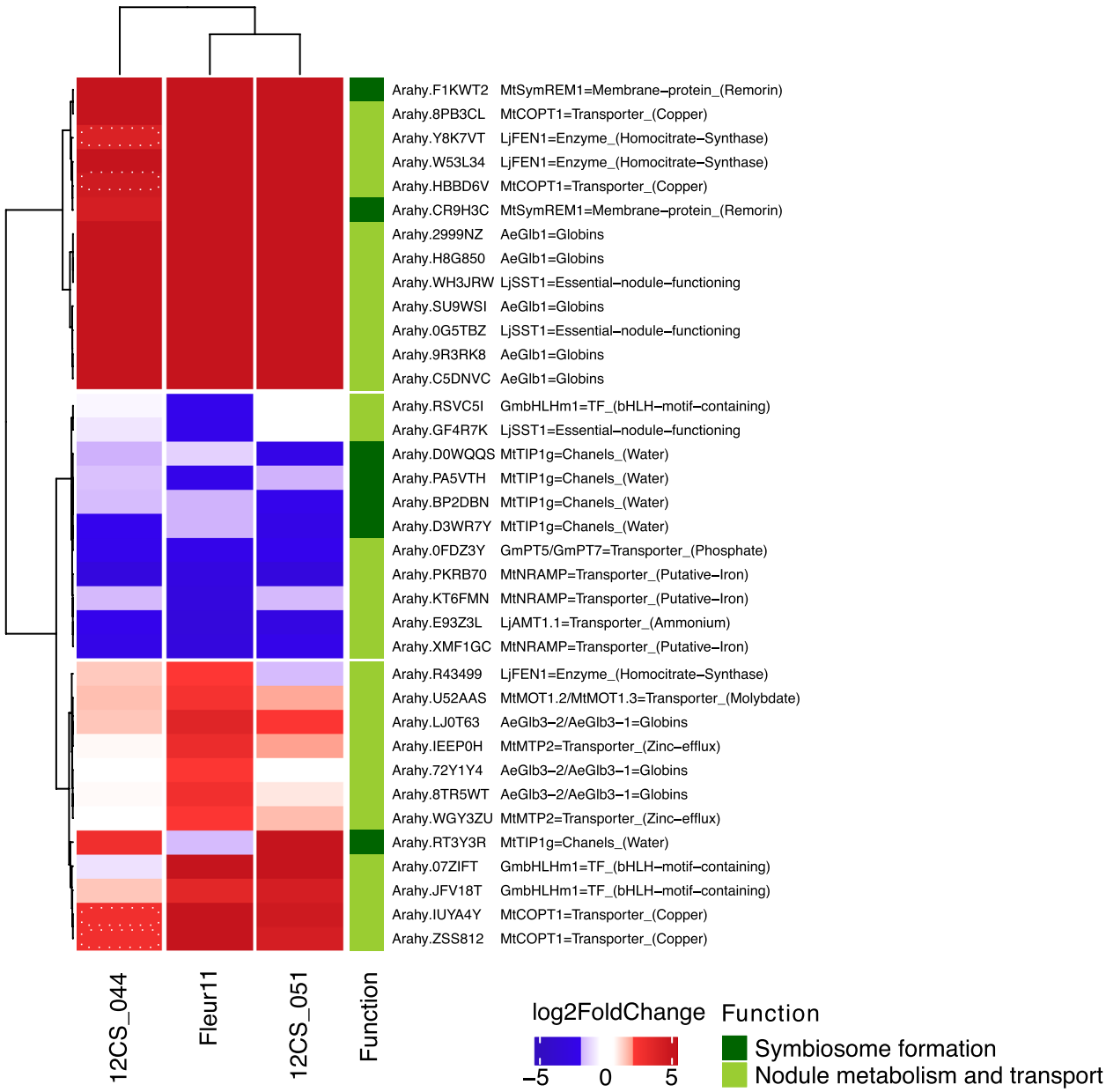

Fig. 5 Comparative analysis of the expression profile of peanut orthologs of symbiotic genes involved in nodule functioning between Fleur11 and the CSSLs. For each genotype, gene expression (log2 FoldChange) was evaluated by comparing the inoculated treatment (21 dpi) with the control (0 dpi, uninoculated). A gene was considered to be differentially expressed if the absolute value of log2 FoldChange ^{3} 2 and the *p*-value £ 0.05. Up and down regulated genes were indicated in red and blue, respectively. The white dotted lines indicate gene that have a fold change greater than the specified threshold but with a non-significant *p*-value

are syntenic (Fig. S6). Among the annotated genes found on these QTLs, orthologs of 10 symbiotic genes were identified on chromosome A02, while 06 orthologs were found on chromosome B02 (Table 3).

We compared the expression of those genes between Fleur11 and the two CSSLs. We identified 67 DEGs situated in the QTL region on chromosome A02 in Fleur11, of which 37 were downregulated and 30 were upregulated. In line 12 CS_051, we found 21 DEGs, with 09 downregulated and 12 upregulated (Table S8, Fig. S7). Similarly, in the QTL region on the chromosome B02 we identified 60 DEGs in Fleur11, of which 26 were downregulated and 34 were upregulated. In line 12 CS_044, there were 26 DEGs, with 13 downregulated and 13 upregulated (Table S8, Fig. S8). Interestingly, among the DEGs situated in each QTL region, we found R genes

Table 2 qRT-PCR validation of RNA-seq results

Genes	Genotypes	qRT-PCR			RNA-Seq (TMM counts)			R^2
		0 dpi	12 dpi	21 dpi	0 dpi	12 dpi	21 dpi	
Arahy.4RTA8 J (*AhAglAG12*)	Fleur11	1	135.46	196.09	0	1444.99	4095.89	0.86
	12 CS_051	1	539.32	1345.19	0	601.29	2648.36	0.96
	12 CS_044	1	0.97	1.75	0.72	2.92	128.96	0.99
Arahy.8L903M	Fleur11	1	14.43	123.33	0	4433.19	6412.84	0.64
	12 CS_051	1	81.81	196.78	0	2125.28	7256.66	0.98
	12 CS_044	1	1.53	5.12	0.37	7.82	191.79	0.99
Arahy.Y8 K7 VT (*AhFEN1*)	Fleur11	1	3.50	39.13	0	222.51	1844.99	0.99
	12 CS_051	1	7.95	66.00	0	59.29	568.01	1.00
	12 CS_044	1	2.17	3.59	2.59	1.87	32.60	0.77
Arahy.R43499 (*AhFEN1*)	Fleur11	1	0.61	0.62	5.16	14.37	13.90	0.99
	12 CS_051	1	0.84	0.63	188.50	60.22	48.85	0.73
	12 CS_044	1	0.76	2.17	12.51	4.63	24.25	0.93
Arahy.B4MRFB (*AhMOT1.2*)	Fleur11	1	2.73	2.61	495.91	3116.47	1242.18	0.58
	12 CS_051	1	2.02	3.86	1015.57	2147.44	3083.87	0.95
	12 CS_044	1	0.89	3.36	769.92	18.56	1644.38	0.81
Arahy.I65 W25 (*AhNIN*)	Fleur11	1	1.30	4.60	119.15	1185.18	3729.47	0.95
	12 CS_051	1	1.35	3.99	169.53	653.00	1547.78	0.94
	12 CS_044	1	2.28	3.00	128.22	54.12	181.58	0
Arahy.IUYB4 A (*AhCRE1*)	Fleur11	1	1.75	0.20	2576.64	4416.04	381.37	0.99
	12 CS_051	1	1.55	0.63	3409.96	2549.10	2068.29	0
	12 CS_044	1	0.44	0.90	3376.13	207.18	1718.04	0.86

dpi indicates days post-inoculation. For qRT-PCR analysis, the expression of each gene was calculated using the comparative threshold cycle method. TMM counts refer to raw read counts normalized using the Trimmed Mean of M-values (TMM) method. TMM counts correspond to quantification of gene expression by RNA-Seq. R^2 indicates the correlation between qRT-PCR and RNA-Seq data

(TIR-NBS-LRR class, encoding resistance proteins) that exhibited different expression levels between the corresponding line and Fleur11 (Table S8, Fig. S7 and S8).

Regarding orthologs of SNF-related genes situated within the QTL regions, we found no differentially expressed genes between the uninoculated treatment and the inoculated treatment at 21 dpi in the chromosome A02 for line 12 CS_051 or in the chromosome B02 for line 12 CS_044. In contrast, we identified two orthologs of *FEN1* (*Arahy.R43499* on chromosome A02 and *Arahy.Y8 K7 VT* on chromosome B02) that were induced in Fleur11 between 0 and 21 dpi (Fig. 6). *FEN1* is involved in nodule metabolism and transport, particularly in the activity of nitrogenase. Notably, the expression of *Arahy.R43499* was at least twofold lower in 12 CS_051 compared to Fleur11. The expression of *Arahy.Y8 K7 VT* was at least threefold lower in line 12 CS_044 compared to Fleur11. Interestingly, *Arahy.Y8 K7 VT* transcript levels were three times more abundant in line 12 CS_051 compared to line 12 CS_044. Additionally, although the expression of *Arahy.R43499* in 12 CS_044 was not statistically significant, we did observe a 1.30-fold increase when compared to 12 CS_051.

Discussion

In this study, we performed a comparative analysis of transcriptomic profiles of two CSSLs impaired for nitrogen fixation, 12 CS_051 and 12 CS_044 and their recurrent parent, Fleur11, aiming to identify signaling pathways and candidate gene(s) associated with the symbiotic phenotypes observed in these two CSSLs. The CSSLs harbor large homeologous wild introgressions on chromosomes A02 and B02 [7], which were associated with the disruption of root-nodule symbiosis process. Plants used in this study exhibited previously described features including low levels of chlorophyll content and abnormal nodule development [8].

Recurrent parent Fleur11, showed a transcriptome prolife similar to previously reported transcriptome of peanut during SNF

As previously described in transcriptome analysis of other peanut accessions at the functional nodule stage (21 dpi) [26, 27], gene functions related to "heme binding", "iron binding", "response to biotic stimulus", "oxygen transport", "response to oxidative stress", "defense

Table 3 Identification of orthologs of previously known SNF-related genes present in QTLs regions corresponding to the QTLs on chromosome A02 and B02

Chr	Gene ID	Orthologs			Function
		M. truncatula	***A. hypogaea***	***A. duranensis/ A. ipaensis***	
A02	*MtLAX2*	MtrunA17_Chr7 g0241841	*Arahy.974 NLB*	*Aradu.ZM0 JI*	Nodule organogenesis
	MtNOOT	MtrunA17_Chr1 g0171771	*Arahy.D2XTM9*	*Aradu.31ZLJ*	
	GmARF8a/8b	MtrunA17_Chr5 g0433301	*Arahy.TZ3SVZ*	*Aradu.STB9 F*	
	MtSCARN	MtrunA17_Chr4 g0004861	*Arahy.ENX9PF*	*Aradu.Z3EUJ*	Rhizobial infection
	MtVAMP721	MtrunA17_Chr2 g0291651	*Arahy.3 N3RG9* *Arahy.JUA6LJ*	*Aradu.3XT84* *Aradu.Q6 WYU*	Symbiosome formation
	MtSymREM1	MtrunA17_Chr8 g0386521	*Arahy.E67BSD*	-	
	LjFEN1	MtrunA17_Chr7 g0226821	*Arahy.SVFK59*	*Aradu.0 A06I*	Nodule metabolism and transport
		MtrunA17_Chr1 g0213481	*Arahy.R43499*	*Aradu.F9 JCM* *Aradu.TP8 FN*	
	LjAMT1.1	MtrunA17_Chr1 g0168631	*Arahy.E0EAR0*	*Aradu.KH25 W*	
	GmPT5	MtrunA17_Chr7 g0261231	*Arahy.XB7U2 C*	*Aradu.ZC0SW Aradu.E3REX*	
	MtFER3	MtrunA17_Chr4 g0005581	*Arahy.MAQ2UP*	*Aradu.N8 FJN*	Senescence
B02	*MtLAX2*	MtrunA17_Chr7 g0241841	*Arahy.B2YEC9*	*Araip.TU273*	Nodule organogenesis
	MtNOOT	MtrunA17_Chr1 g0171771	*Arahy.K4 FBU4*	*Araip.RJS33*	
	MtSCARN	MtrunA17_Chr4 g0004861	*Arahy.6 AJ8U6*	*Araip.0SG8 W*	Rhizobial infection
	LjFEN1	MtrunA17_Chr7 g0226821	*Arahy.I9 TRT4* *Arahy.T5GDAR*	*Araip.82ZQZ* *Araip.N3U2H*	Nodule metabolism and transport
		MtrunA17_Chr1 g0213481	*Arahy.14SFHV* *Arahy.I3BSCY* *Arahy.Y8 K7 VT*	*Araip.J9L15* *Araip.VLA9D* *Araip.X1RXQ*	
	MtFER3	MtrunA17_Chr4 g0005581	*Arahy.B2GHU0*	*Araip.S9G3 C*	Senescence
	GmBEHL1	MtrunA17_Chr5 g0403631	*Arahy.ZGY2QD*	*Araip.C7RCE*	Autoregulation of nodule number

Chr Chromosome

response to bacterium", "oxidoreduction activity", "O-glycosyl hydrolase activity" and "DNA transcription" were particularly over-represented among the DEGs identified in Fleur11. The peanut orthologs of nodule-specific expressed genes, including *Glb1/AhSymH1-3*, *SST1*, *AglAG12* and *CAPs*, were among the highly expressed genes. Furthermore, peanut orthologs of key SNF-related genes such *NIN*, *EFD*, *FEN1*, *RR5/9/11* and nodule-induced transporters genes were upregulated in Fleur11. Similar results were described not only in other peanut accessions [26, 27], but also in other nitrogen-fixing species particularly for genes such as *NIN*, *Glb1*, *SST1* and *AglAG12* [28]. We conclude that in our conditions, the transcriptome of Fleur11 plants infected by ISRA400 *B. vignae* strain shows the same patterns previously described for other peanut accessions in interaction with other rhizobial strains. However, thanks to our Orthofinder analysis we were able to include the expression analysis of many orthologs of symbiotic genes that were not considered in previous studies [23, 26, 27].

Expression of plant immunity and symbitotic genes reflects the phenotypic differences between CSSLs and Fleur11

Genes related to plant immunity were expressed differentially in the CSSLs compared to Fleur11. Several genes involved in protein kinase activities or defense response were significantly upregulated only in the two CSSLs. Protein kinases play a crucial role in pattern triggered immunity pathway during pathogen recognition and subsequent induction of plant defense mechanisms, including the activation of transcription factors and systemic responses [53]. This suggest that the induction of these genes may have led to the recognition of rhizobia as a pathogen, triggering defense responses that arrest further rhizobial invasion and eliminate ineffective nodules. The presence of necrosed tissues and/or high proportion dead bacteria in nodule sections of the CSSLs [8] supports this idea. Interestingly, transcriptome profiles revealed that genes encoding nodule-specific cysteine-rich proteins and peptides (*CAPs* and *NCRs*), exhibited lower expression levels in the two CSSLs compared to

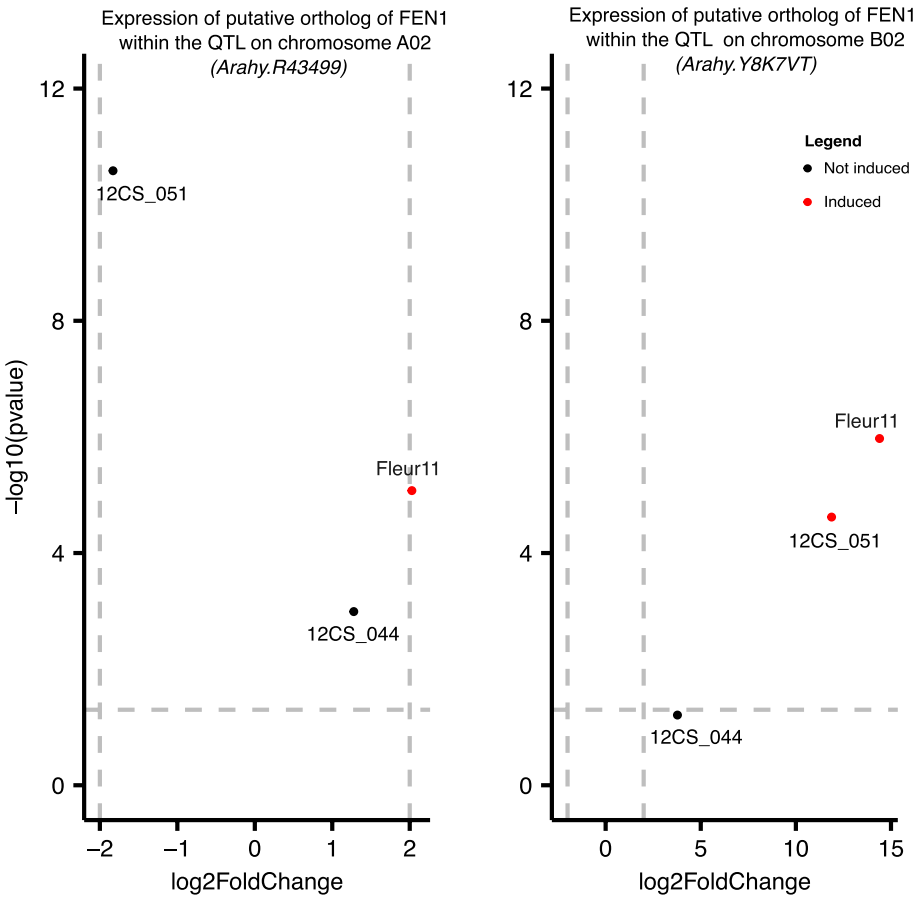

Fig. 6 Volcano plots of expression for *FEN1* orthologs highlighting significance ($p \leq 0.05$) and gene expression thresholds (log2 FoldChange ≤ -2 or ≥ 2) across genotypes

Fleur11. As observed in Fleur11, high expression of *CAPs* and *NCRs* has been previously linked to efficient nitrogen fixation in peanut [26, 27], and other legumes such as *Aeschynomene evenia* [52, 54], and pea [55]. The role of cysteine-rich proteins in legume-rhizobia symbiosis is still not completely understood. Given their broad range of potent antimicrobial activities [56, 57], it is assumed that these proteins may play a role in inhibiting plant defense mechanisms and regulating terminal rhizobial differentiation. In *M. truncatula*, the lack in expression of some NCR-encoding genes inhibits bacteria differentiation and leads to severe symptoms of impaired nitrogen fixation, such as senescence of nodules and death of rhizobia inside nodules [58, 59].

In addition, some orthologs of chalcone synthase and reductase (*CHS* and *CHR*), involved in flavonoid biosynthesis were induced at 21 dpi only in the CSSLs compared to Fleur11. At the early stage of legume symbiosis, flavonoids play a crucial role as symbiotic signal molecules promoting the formation of nodules [60, 61], whereas their expression at the late stages is possibly related to their role in defense mechanisms [62]. Indeed, once rhizobial infection has occurred, flavonoid induction is not required during determinate nodule formation in compatible symbiosis interactions [63]. On the other hand, it was reported that most of genes involved in plant immunity such as those involved in the jasmonic acid signaling pathway, were notably downregulated during SNF in peanut [26]. In contrast, the gene encoding for jasmonate-zim-domain (JAZ) protein 1 exhibited the highest expression level in line 12 CS_044. JAZ proteins are known as the key regulators of jasmonate signaling, an important integrator of plant–microbe interactions [64]. The involvement of JAZ proteins in root nodules symbiosis was demonstrated in peanut [65]. The analysis of the expression pattern of JAZ genes at different time points of peanut nodulation showed an enhanced expression during the early stage (4–8 dpi), which decreased considerably at later stage (12–30 dpi) [26, 65]. Moreover, while the two QTLs contain orthologs of R and SNF-related genes which are differentially expressed between the CSSLs and Fleur11, there is no clear evidence to

suggest that changes in gene expression related to plant immunity is either the cause or consequence of impaired nitrogen fixation observed in the CSSLs.

At the mature nodule stage, we found 154 peanut orthologs corresponding to 33 genes involved in nodule functioning during symbiosis in model legumes. The large number of orthologs found in the peanut genome is linked to tetraploidization and subsequent gene duplication events. In Fleur11, most of genes encoding SNF-related transporters are induced at the functional nodule stage, similarly to previous results obtained in others peanut accessions [27]. In contrast, we found that some orthologs of genes encoding SNF-related transporters such as, *MTP2* [66], *Glb3-2* [52], *MOT1.2* [67], *GmbHLm1* [68] showed low levels of expression in the two CSSLs. The lack of nodule induced transcripts of SNF-related transporter genes can impair bacteria differentiation, and lead to severe reductions in nodule fitness and nitrogenase activity.

Remarkably, some orthologs of *FEN1* were not induced at 21 dpi in the two CSSLs compared to Fleur11. Previous studies have demonstrated that *fen1* mutants fail to enlarge infected cells and form white nodules that are unable to fix efficiently nitrogen in *L. japonicus* [69–71]. On the other hand, the lines 12 CS_051 and 12 CS_044 produced nodules that were, respectively, slightly smaller and very small in comparison to those of Fleur11, as previously described [8]. Nodule size is possibly related to the expression levels of genes related to organogenesis. Most of the key transcription factors required for nodule organogenesis were upregulated in Fleur11 at 21 dpi. In contrast, even the master regulator gene, *NIN*, was induced in line 12 CS_051, other transcriptions factors, including ethylene response factor required for nodule differentiation (*EFD*) [72] and response regulator (*RR5/9/11*) [73] were not significantly induced. The lack of induction of these genes leads to the inhibition of cytokinin signaling, which in turn affects the nodule development and suppresses the initiation of new nodules in *M. truncatula*. In the line 12 CS_044, we found that *NIN*, *EFD* and *RR5/9/11* orthologs were not significantly induced, and this is possibly related to the pronounced reduction in nodule size observed in this line. Indeed, a defective expression of *NIN* is known to affect rhizobial infection, nodule number and development [74]. Interestingly, the analysis of transcriptome profiles at 12 dpi, revealed that in the CSSLs, *NIN*, *EFD* and *RR5/9/*11 are expressed at similar levels compared to that observed to 21 dpi (Table S6, Fig.S9). These finding suggest that the phenotypic and transcriptomic variations observed at the functional nodule stage may be a consequence of a deficiency manifested at the early stages. This implies that the symbiotic process could be blocked at the organogenesis stage in the CSSLs. Assuming that the gene(s) responsible of phenotypic and transcriptomic variations are located within the wild introgression carried by each line, we can investigate the hypothesis outlined above.

A candidate gene potentially involved in SNF was found in the homoeologous QTLs on chromosomes A02 and B02

It clearly appears that homeologous QTLs on chromosomes A02 and B02 have different effects on SNF-related traits and expression of SNF-related genes in the corresponding line. These finding may be attributed to various genetic factors, such as gene dosage effects, allelic interactions, functional divergence (neo-functionalization) of genes, redundancy or compensation (sub-functionalization) of genes. Changes in gene expression of homeologous QTLs, leading to various phenotypic effects have been extensively reported in allopolyploids, such as wheat and cotton [75]. In the two targeted regions on chromosomes A02 and B02, we found two orthologs of *FEN1*, *Arahy.R43499* and *Arahy.Y8 K7 VT*, respectively, which were induced in Fleur11, but not in the corresponding line. The ortholog *Arahy.Y8 K7 VT* is known to be expressed only nodules in peanut [27]. *FEN1* encodes for a homocitrate synthase, which is an essential cofactor provided by the legume, to activate the nitrogenase of rhizobia [69, 76]. In *L. japonicus*, the lack of nodule-specific *FEN1* expression in fen1 mutants leads to nitrogen deficiency symptoms, including the formation of small, pale and pink nodules that are infected by differentiated bacteria but do not fix nitrogen (Fix-) [69]. It was demonstrated that, *FEN1* overcomes the lack of rhizobial homocitrate synthase (*NifV*) during the symbiosis with *Mesorhizobium loti* [69]. However, *NifV* is not present in most rhizobia that can establish efficient SNF [76]. Nevertheless, there is no clear evidence to prove that the presence of *NifV* gene is related to the absence of *FEN1* expression in legume-rhizobia symbiosis. The efficient *B. vignae* ISRA400 strain used as inoculum in this study contains a *NifV* gene [77], while the efficient *Bradyrhizobium* sp. SEMIA6144, used as inoculum in previous studies in peanut [26, 27], does not. Interestingly, both strains form efficient nitrogen fixing nodules and *FEN1* shows high level of expression in *A. hypogaea* [27]. Taken together, these results suggest that *FEN1* could be essential for rhizobial nitrogenase activity in peanut-Bradyrhizobium symbiosis and can be a suitable candidate gene to explain phenotypic variations observed in the two CSSLs. We hypothesize that the lack of expression of one *FEN1* ortholog may impair nitrogenase activity, thereby contributing to nitrogen fixation deficiency observed in the CSSLs. The expression of the two orthologs of *FEN1* in the CSSLs compared to

Fleur11, coupled with the observed differences in phenotypes, suggest distinct or complementary gene functions. This hypothesis is supported by the RNA-Seq analysis at nodule development stage (12 dpi), which showed that *Arahy.Y8 K7 VT* was induced only in Fleur11 and line 12 CS_051, whereas *Arahy.R43499* was not differentially expressed in all genotypes (Table S3). *Arahy.Y8 K7 VT* appears to be involved in downstream stages of symbiosis such as nodule organogenesis. A significant increase in the expression of *Arahy.Y8 K7 VT* was reported at 10 dpi during symbiosis in peanut [27]. Moreover, a mutation that could potentially alter protein function was found between the coding sequences of *Arahy.R43499* from the available *A. hypogaea* and *A. duranensis* genomes (from PeanutBase). While, for the coding sequences of *Arahy.Y8 K7 VT*, no difference was found between the *A. hypogaea* and *A. ipaensis* genomes (Fig. S10). These findings suggest that the lack of expression of *FEN1* orthologs in the CSSLs, compared to Fleur11, could be linked to changes in the regulatory sequence (promoter or enhancer/silencer) of the corresponding ortholog. Interestingly, although the promoter regions of *Arahy.R43499* and *Aradu.TP8 FN* are almost identical, a "CTCTT" motif characteristic of the promoters that are activated in nodules [78, 79] is only present in the promoter regions of *Arahy.R43499* (Fig. S11a).

To investigate and validate the role of plant homocitrate (*FEN1*) in the phenotypic characteristics observed in the CSSLs, it would be valuable to carry out a fine mapping experiment by developing near-isogenic lines. This approach would allow to refine QTL regions and facilitate the validation of candidate gene within these narrowed QTL regions [80–83]. Additionally, genome editing techniques, such as CRISPIR/Cas9 could be used together with hairy root transformation to target peanut orthologs of *FEN1* located in the QTL regions in loss of function or swapping gene experiments [32, 84–87]. These genetic approaches could be combined with assessments on the ability of *B. vignae* ISRA400 to fix nitrogen in their free-living state, and to form efficient nitrogen-fixing nodules, even in the absence of the *NifV* gene. A summary highlighting *FEN1* as a suitable candidate gene for the phenotype observed in CSSLs, along with the genetic approaches to investigate its role during peanut SNF, are provided in Supplementary Figure S12.

Conclusion

Homoeologous wild introgressions/QTLs harbored by the two CSSLs negatively affect the process of SNF, and this is reflected in significant differences in the expression of genes involved particularly in plant immune signaling and symbiosis. The changes in transcriptome profiles support a specific effect of these QTLs in SNF process. Of particular interest, two orthologs of *FEN1* located on chromosome A02 and chromosome B02 are the suitable candidate genes to explain the phenotypic characteristics caused by these introgressions.

Abbreviations

SNF	Symbiotic nitrogen fixation
CSSL	Chromosome substitution segment line
QTL	Quantitative trait loci
NFs	Nod factors
TF	Transcription factor
dpi	Days post-inoculation
SPAD	Soil plant analysis development
CERAAS	Centre de recherche pour l'amélioration de l'adadptation à la sécheresse
LCM	Laboratoire commun de microbiologie
DEG	Differentially expressed genes
GO	Gene ontology

Supplementary Information

The online version contains supplementary material available at https://doi.org/10.1186/s12864-025-11739-y.

Supplementary Material 1. Supplementary figures.

Supplementary Material 2: Table S1. Primers of genes used for qRT-PCR.

Supplementary Material 3: Table S2. Gene Ontology enrichment of DEGs identified in Fleur11 at 12 and 21 days post inoculation.

Supplementary Material 4: Table S3. Differentially expressed genes identified in all the genotypes at 12 and 21 days post inoculation.

Supplementary Material 5: Table S4. Gene ontology enrichment of DEGs identified especially in each genotype by comparing each line with Fleur11.

Supplementary Material 6: Table S5. Identification of peanut orthologs of symbiotic genes.

Supplementary Material 7: Table S6. Identification of peanut orthologs of symbiotic genes differentially expressed in all genotypes at 12 and 21 days post inoculation.

Supplementary Material 8: Table S7. Identification of defensin-like nodule-specific cysteine rich peptides (NCRs) and cysteine-rich secretory proteins, antigen 5, and pathogenesis-related 1 proteins(CAPs) differentially expressed in all genotypes at 21 days post inoculation.

Supplementary Material 9: Table S8. Identification of DEGs on the QTLs on chromosomes A02 and B02.

Acknowledgements

The authors thank Dr Fabienne Cartieaux for valuable suggestions during the finalization of the manuscript.

Authors' contributions

D.T.N., D.F., S.F. and S.S. designed the experiments, D.T.N. M.C., D.G., V.H. contributed to RNA-Seq and qRT-PCR analysis. D.T.N. wrote the original draft manuscript, V.H., J-F.R., S.F, D.F. and S.S. significantly contributed on writing manuscript. All the authors reviewed and approved the final manuscript.

Funding

The work was funded by Institut de Recherche pour le Développement (IRD) through the Laboratoire Mixte International Adaptation des Plantes et microorganisms associés aux stress Environnementaux (LMI LASPE). Darius T. Nzepang's PhD grant was founded by the German Academic Exchange Service (DAAD), the Avril Foundation (ORACLE project) and the IRD Research Allowance for a Southern Thesis (ARTS). Additionally, his post-doctoral contract was supported by the Agropolis Foundation (Div-N-Fix project).

Data availability
The datasets generated and analyzed in the current study are available in the NCBI Gene Expression Omnibus (GEO) under accession number GSE289879. https://www.ncbi.nlm.nih.gov/geo/query/acc.cgi?acc=GSE289879.

Declarations

Ethics approval and consent to participate
Not applicable.

Consent for publication
Not applicable.

Competing interests
The authors declare no competing interests.

Author details
[1]Centre d'Etudes Régional Pour L'Amélioration de L'Adaptation À La Sécheresse, CERAAS-Route de Khombole, Thiès BP3320, Senegal. [2]Laboratoire Commun de Microbiologie (LCM) (IRD/ISRA/UCAD), Centre de Recherche de Bel Air, Dakar BP1386, Senegal. [3]PHIM Plant Health Institute, Univ Montpellier, IRD, CIRAD, INRAE, Institut Agro, Montpellier, France. [4]CIRAD, UMR AGAP, Montpellier 34398, France. [5]AGAP, Univ Montpellier, CIRAD, INRAE, Institut Agro, Montpellier, France.

Received: 18 March 2025 Accepted: 21 May 2025
Published online: 03 June 2025

References

1. Bertioli DJ, Cannon SB, Froenicke L, Huang G, Farmer AD, Cannon EKS, et al. The genome sequences of Arachis duranensis and Arachis ipaensis, the diploid ancestors of cultivated peanut. Nat Genet. 2016;48:438–46.
2. Hardarson G. Methods for enhancing symbiotic nitrogen fixation. Plant Soil. 1993;152:1–17.
3. Herridge DF, Peoples MB, Boddey RM. Global inputs of biological nitrogen fixation in agricultural systems. Plant Soil. 2008;311:1–18.
4. Jaiswal SK, Msimbira LA, Dakora FD. Phylogenetically diverse group of native bacterial symbionts isolated from root nodules of groundnut (Arachis hypogaea L.) in South Africa. Syst Appl Microbiol. 2017;40:215–26.
5. Zaiya ZA, Fonceka D, Fall S, Fabra A, Ibañez F, Pignoly S, et al. Genetic diversity and symbiotic efficiency of rhizobial strains isolated from nodules of peanut (Arachis hypogaea L.) in Senegal. Agric Ecosystems Environ. 2018;265:384–91.
6. Brooker RW, Bennett AE, Cong W-F, Daniell TJ, George TS, Hallett PD, et al. Improving intercropping: a synthesis of research in agronomy, plant physiology and ecology. New Phytol. 2015;206:107–17.
7. Fonceka D, Tossim H-A, Rivallan R, Vignes H, Lacut E, de Bellis F, et al. Construction of chromosome segment substitution lines in peanut (Arachis hypogaea L.) using a wild synthetic and QTL mapping for plant morphology. PLOS One. 2012;7:e48642.
8. Nzepang DT, Gully D, Nguepjop JR, ZaiyaZazou A, Tossim HA, Sambou A, et al. Mapping of QTLs associated with biological nitrogen fixation traits in peanuts (Arachis hypogaea L.) using an interspecific population derived from the cross between the cultivated species and its wild ancestors. Genes. 2023;14:797.
9. Ibáñez F, Wall L, Fabra A. Starting points in plant-bacteria nitrogen-fixing symbioses: intercellular invasion of the roots. J Exp Bot. 2017;68:1905–18.
10. Quilbé J, Montiel J, Arrighi J-F, Stougaard J. Molecular mechanisms of intercellular Rhizobial infection: novel findings of an ancient process. Front Plant Sci. 2022;13(13):922982.
11. Oldroyd GED. Speak, friend, and enter: signalling systems that promote beneficial symbiotic associations in plants. Nat Rev Microbiol. 2013;11:252–63.
12. Oldroyd GED, Murray JD, Poole PS, Downie JA. The rules of engagement in the legume-rhizobial symbiosis. Annu Rev Genet. 2011;45:119–44.
13. Roy S, Liu W, Nandety RS, Crook A, Mysore KS, Pislariu CI, et al. Celebrating 20 years of genetic discoveries in legume nodulation and symbiotic nitrogen fixation. Plant Cell. 2020;32:15–41.
14. Redmond JW, Batley M, Djordjevic MA, Innes RW, Kuempel PL, Rolfe BG. Flavones induce expression of nodulation genes in Rhizobium. Nature. 1986;323:632–5.
15. Høgslund N, Radutoiu S, Krusell L, Voroshilova V, Hannah MA, Goffard N, et al. Dissection of symbiosis and organ development by integrated transcriptome analysis of lotus japonicus mutant and wild-type plants. PLoS One. 2009;4:e6556.
16. Yuan S, Li R, Chen S, Chen H, Zhang C, Chen L, et al. RNA-seq analysis of differential gene expression responding to different rhizobium strains in soybean (Glycine max) roots. Front Plant Sci. 2016;7:721.
17. Yuan SL, Li R, Chen HF, Zhang CJ, Chen LM, Hao QN, et al. RNA-seq analysis of nodule development at five different developmental stages of soybean (Glycine max) inoculated with Bradyrhizobium japonicum strain 113–2. Sci Rep. 2017;7:42248.
18. Shi Y, Zhang Z, Wen Y, Yu G, Zou J, Huang S, et al. RNA sequencing-associated study identifies GmDRR1 as positively regulating the establishment of symbiosis in soybean. MPMI. 2020;33:798–807.
19. Keller J, Imperial J, Ruiz-Argüeso T, Privet K, Lima O, Michon-Coudouel S, et al. RNA sequencing and analysis of three *Lupinus* nodulomes provide new insights into specific host-symbiont relationships with compatible and incompatible *Bradyrhizobium* strains. Plant Sci. 2018;266:102–16.
20. Kamfwa K, Zhao D, Kelly JD, Cichy KA. Transcriptome analysis of two recombinant inbred lines of common bean contrasting for symbiotic nitrogen fixation. PLoS One. 2017;12:e0172141.
21. Bertioli DJ, Jenkins J, Clevenger J, Dudchenko O, Gao D, Seijo G, et al. The genome sequence of segmental allotetraploid peanut Arachis hypogaea. Nat Genet. 2019;51:877–84.
22. Zhuang W, Chen H, Yang M, Wang J, Pandey MK, Zhang C, et al. The genome of cultivated peanut provides insight into legume karyotypes, polyploid evolution and crop domestication. Nat Genet. 2019;51:865–76.
23. Peng Z, Liu F, Wang L, Zhou H, Paudel D, Tan L, et al. Transcriptome profiles reveal gene regulation of peanut (Arachis hypogaea L.) nodulation. Sci Rep. 2017;7:1–12.
24. Lu Q, Li H, Hong Y, Zhang G, Wen S, Li X, et al. Genome sequencing and analysis of the peanut B-genome progenitor (Arachis ipaensis). Front Plant Sci. 2018;9:604.
25. Griesmann M, Chang Y, Liu X, Song Y, Haberer G, Crook MB, et al. Phylogenomics reveals multiple losses of nitrogen-fixing root nodule symbiosis. Science. 2018;361:eaat1743.
26. Karmakar K, Kundu A, Rizvi AZ, Dubois E, Severac D, Czernic P, et al. Transcriptomic analysis with the progress of symbiosis in 'crack-entry' legume arachis hypogaea highlights its contrast with 'infection thread' adapted legumes. MPMI. 2018;32:271–85.
27. Raul B, Bhattacharjee O, Ghosh A, Upadhyay P, Tembhare K, Singh A, et al. Microscopic and transcriptomic analyses of dalbergoid legume peanut reveal a divergent evolution leading to nod-factor-dependent epidermal crack-entry and terminal bacteroid differentiation. MPMI. 2022;35:131–45.
28. Zhang Y, Fu Y, Xian W, Li X, Feng Y, Bu F, et al. Comparative phylogenomics and phylotranscriptomics provide insights into the genetic complexity of nitrogen-fixing root-nodule symbiosis. Plant Comm. 2024;5:100671.
29. Sinharoy S, DasGupta M. RNA interference highlights the role of CCaMK in dissemination of endosymbionts in the aeschynomeneae legume arachis. MPMI. 2009;22:1466–75.
30. Kundu A, DasGupta M. Silencing of putative cytokinin receptor Histidine Kinase1 inhibits both inception and differentiation of root nodules in arachis hypogaea. Mol Plant Microbe Interact. 2018;31:187–99.
31. Das DR, Horváth B, Kundu A, Kaló P, DasGupta M. Functional conservation of CYCLOPS in crack entry legume Arachis hypogaea. Plant Sci. 2019;281:232–41.
32. Shu H, Luo Z, Peng Z, Wang J. The application of CRISPR/Cas9 in hairy roots to explore the functions of AhNFR1 and AhNFR5 genes during peanut nodulation. BMC Plant Biol. 2020;20:417.
33. Peng Z, Chen H, Tan L, Shu H, Varshney RK, Zhou Z, et al. Natural polymorphisms in a pair of NSP2 homoeologs can cause loss of nodulation in peanut. J Exp Bot. 2021;72:1104–18.
34. Somasegaran P, Hoben HJ. Handbook for Rhizobia: methods in legume-rhizobium technology. New York: Springer-Verlag; 1994.

35. Ehrhardt DW, Atkinson EM, Long SR. Depolarization of alfalfa root hair membrane potential by Rhizobium meliloti Nod factors. Science. 1992;256:998–1000.
36. Hothorn T, Bretz F, Westfall P. Simultaneous inference in general parametric models. Biom J. 2008;50:346–63.
37. Martin M. Cutadapt removes adapter sequences from high-throughput sequencing reads. EMBnet J. 2011;17:10–2.
38. Ewels PA, Peltzer A, Fillinger S, Patel H, Alneberg J, Wilm A, et al. The nf-core framework for community-curated bioinformatics pipelines. Nat Biotechnol. 2020;38:276–8.
39. Patel H, Ewels P, Peltzer A, Hammarén R, Botvinnik O, Sturm G, et al. nf-core/rnaseq: nf-core/rnaseq v3.0 - Silver Shark. Zenodo; 2020.
40. Dobin A, Davis CA, Schlesinger F, Drenkow J, Zaleski C, Jha S, et al. STAR: ultrafast universal RNA-seq aligner. Bioinformatics. 2013;29:15–21.
41. García-Alcalde F, Okonechnikov K, Carbonell J, Cruz LM, Götz S, Tarazona S, et al. Qualimap: evaluating next-generation sequencing alignment data. Bioinformatics. 2012;28:2678–9.
42. Patro R, Duggal G, Love MI, Irizarry RA, Kingsford C. Salmon provides fast and bias-aware quantification of transcript expression. Nat Methods. 2017;14:417–9.
43. Robinson MD, McCarthy DJ, Smyth GK. edgeR: a Bioconductor package for differential expression analysis of digital gene expression data. Bioinformatics. 2010;26:139–40.
44. Yan L. ggvenn: draw venn diagram by "ggplot2." 2023.
45. Gu Z. Complex heatmap visualization. iMeta. 2022;1:e43.
46. Wickham H. ggplot2. Cham: Springer International Publishing; 2016.
47. Young MD, Wakefield MJ, Smyth GK, Oshlack A. Gene ontology analysis for RNA-seq: accounting for selection bias. Genome Biol. 2010;11:R14.
48. Ye J, Zhang Y, Cui H, Liu J, Wu Y, Cheng Y, et al. WEGO 2.0: a web tool for analyzing and plotting GO annotations, 2018 update. Nucleic Acids Res. 2018;46:W71-5.
49. Ye J, Fang L, Zheng H, Zhang Y, Chen J, Zhang Z, et al. WEGO: a web tool for plotting GO annotations. Nucleic Acids Research. 2006;34 suppl_2:W293-7.
50. Emms DM, Kelly S. OrthoFinder: solving fundamental biases in whole genome comparisons dramatically improves orthogroup inference accuracy. Genome Biol. 2015;16:157.
51. van Velzen R, Holmer R, FengJiao B, Rutten L, van Zeijl A, Wei L, et al. Comparative genomics of the nonlegume parasponia reveals insights into evolution of nitrogen-fixing rhizobium symbioses. Proc Natl Acad Sci U S A. 2018;115:E4700.
52. Quilbé J, Lamy L, Brottier L, Leleux P, Fardoux J, Rivallan R, et al. Genetics of nodulation in Aeschynomene evenia uncovers mechanisms of the rhizobium–legume symbiosis. Nat Commun. 2021;12:829.
53. Romeis T. Protein kinases in the plant defence response. Curr Opin Plant Biol. 2001;4:407–14.
54. Czernic P, Gully D, Cartieaux F, Moulin L, Guefrachi I, Patrel D, et al. Convergent evolution of endosymbiont differentiation in dalbergioid and inverted repeat-lacking clade legumes mediated by nodule-specific cysteine-rich peptides. Plant Physiol. 2015;169:1254–65.
55. Zorin EA, Kliukova MS, Afonin AM, Gribchenko ES, Gordon ML, Sulima AS, et al. A variable gene family encoding nodule-specific cysteine-rich peptides in pea (Pisum sativum L.). Front Plant Sci. 2022;13:884726.
56. Maróti G, Downie JA, Kondorosi É. Plant cysteine-rich peptides that inhibit pathogen growth and control rhizobial differentiation in legume nodules. Curr Opin Plant Biol. 2015;26:57–63.
57. Breen S, Williams SJ, Outram M, Kobe B, Solomon PS. Emerging insights into the functions of pathogenesis-related protein 1. Trends Plant Sci. 2017;22:871–9.
58. Kim M, Chen Y, Xi J, Waters C, Chen R, Wang D. An antimicrobial peptide essential for bacterial survival in the nitrogen-fixing symbiosis. Proc Natl Acad Sci. 2015;112:15238–43.
59. Horváth B, Domonkos Á, Kereszt A, Szűcs A, Ábrahám E, Ayaydin F, et al. Loss of the nodule-specific cysteine rich peptide, NCR169, abolishes symbiotic nitrogen fixation in the Medicago truncatula dnf7 mutant. Proc Natl Acad Sci. 2015;112:15232–7.
60. Wasson AP, Pellerone FI, Mathesius U. Silencing the flavonoid pathway in Medicago truncatula inhibits root nodule formation and prevents auxin transport regulation by rhizobia. Plant Cell. 2006;18:1617–29.
61. Zhang J, Subramanian S, Stacey G, Yu O. Flavones and flavonols play distinct critical roles during nodulation of Medicago truncatula by Sinorhizobium meliloti. Plant J. 2009;57:171–83.
62. Das A, Choudhury S, Gopinath V, Majeed W, Chakraborty S, Bhairavi KS, et al. Functions of flavonoids in plant, pathogen, and opportunistic fungal interactions. In: MohdS A, editor., et al., Opportunistic fungi, nematode and plant interactions: interplay and mechanisms. Singapore: Springer Nature; 2024. p. 91–123.
63. Subramanian S, Stacey G, Yu O. Distinct, crucial roles of flavonoids during legume nodulation. Trends Plant Sci. 2007;12:282–5.
64. Chini A, Fonseca S, Fernández G, Adie B, Chico JM, Lorenzo O, et al. The JAZ family of repressors is the missing link in jasmonate signalling. Nature. 2007;448:666–71.
65. Sen S, DasGupta M. Involvement of Arachis hypogaea Jasmonate ZIM domain/TIFY proteins in root nodule symbiosis. J Plant Res. 2021;134:307–26.
66. León-Mediavilla J, Senovilla M, Montiel J, Gil-Díez P, Saez Á, Kryvoruchko IS, et al. MtMTP2-facilitated zinc transport into intracellular compartments is essential for nodule development in Medicago truncatula. Front Plant Sci. 2018;9:990.
67. Tejada-Jiménez M, Gil-Díez P, León-Mediavilla J, Wen J, Mysore KS, Imperial J, et al. Medicago truncatula Molybdate Transporter type 1 (MtMOT1.3) is a plasma membrane molybdenum transporter required for nitrogenase activity in root nodules under molybdenum deficiency. New Phytol. 2017;216:1223–35.
68. Chiasson DM, Loughlin PC, Mazurkiewicz D, Mohammadidehcheshmeh M, Fedorova EE, Okamoto M, et al. Soybean SAT1 (Symbiotic Ammonium Transporter 1) encodes a bHLH transcription factor involved in nodule growth and NH4+ transport. Proc Natl Acad Sci U S A. 2014;111:4814–9.
69. Hakoyama T, Niimi K, Watanabe H, Tabata R, Matsubara J, Sato S, et al. Host plant genome overcomes the lack of a bacterial gene for symbiotic nitrogen fixation. Nature. 2009;462:514–7.
70. Kawaguchi M, Imaizumi-Anraku H, Koiwa H, Niwa S, Ikuta A, Syono K, et al. Root, root hair, and symbiotic mutants of the model legume Lotus japonicus. Mol Plant Microbe Interact. 2002;15:17–26.
71. Imaizumi-Anraku H, Kawaguchi M, Koiwa H, Akao S, Syōno K. Two ineffective-nodulating mutants of lotus japonicus—different phenotypes caused by the blockage of endocytotic bacterial release and nodule maturation. Plant Cell Physiol. 1997;38:871–81.
72. Vernié T, Moreau S, de Billy F, Plet J, Combier J-P, Rogers C, et al. EFD Is an ERF transcription factor involved in the control of nodule number and differentiation in Medicago truncatula. Plant Cell. 2008;20:2696.
73. den Op Camp RHM, De Mita S, Lillo A, Cao Q, Limpens E, Bisseling T, et al. A phylogenetic strategy based on a legume-specific whole genome duplication yields symbiotic cytokinin type-A response regulators. Plant Physiol. 2011;157:2013–22.
74. Schauser L, Roussis A, Stiller J, Stougaard J. A plant regulator controlling development of symbiotic root nodules. Nature. 1999;402:191–5.
75. Adams KL. Evolution of duplicate gene expression in polyploid and hybrid plants. J Hered. 2007;98:136–41.
76. Nouwen N, Arrighi J-F, Cartieaux F, Chaintreuil C, Gully D, Klopp C, et al. The role of rhizobial (NifV) and plant (FEN1) homocitrate synthases in Aeschynomene/photosynthetic Bradyrhizobium symbiosis. Sci Rep. 2017;7:448.
77. Niang D, Gueddou A, Niang N, Nzepang D, Sambou A, Diouf A, et al. Permanent draft genome sequence of Bradyrhizobium vignae, strain ISRA 400, an elite nitrogen-fixing bacterium, isolated from the groundnut growing area in Senegal. J Genomics. 2023;11:52–7.
78. Vieweg MF, Frühling M, Quandt HJ, Heim U, Bäumlein H, Pühler A, et al. The promoter of the Vicia faba L. leghemoglobin gene VfLb29 is specifically activated in the infected cells of root nodules and in the arbuscule-containing cells of mycorrhizal roots from different legume and nonlegume plants. Mol Plant Microbe Interact. 2004;17:62–9.
79. Fehlberg V, Vieweg MF, Dohmann EMN, Hohnjec N, Pühler A, Perlick AM, et al. The promoter of the leghaemoglobin gene VfLb29: functional analysis and identification of modules necessary for its activation in the infected cells of root nodules and in the arbuscule-containing cells of mycorrhizal roots. J Exp Bot. 2005;56:799–806.
80. Alyr MH, Pallu J, Sambou A, Nguepjop JR, Seye M, Tossim HA, et al. Fine-mapping of a wild genomic region involved in pod and seed size

reduction on chromosome A07 in peanut (Arachis hypogaea L.). Genes. 2020;11:1402.
81. Brouwer DJ, St Clair DA. Fine mapping of three quantitative trait loci for late blight resistance in tomato using near isogenic lines (NILs) and sub-NILs. Theor Appl Genet. 2004;108:628–38.
82. Tang F, Yang S, Liu J, Gao M, Zhu H. Fine mapping of the Rj4 locus, a gene controlling nodulation specificity in soybean. Mol Breeding. 2014;33:691–700.
83. Jaganathan D, Bohra A, Thudi M, Varshney RK. Fine mapping and gene cloning in the post-NGS era: advances and prospects. Theor Appl Genet. 2020;133:1791–810.
84. Singh S, Sangh C, Kona P, Bera SK. Genome editing in peanuts: advancements, challenges and applications. Nucleus. 2024;67:127–39.
85. Han HW, Yu ST, Wang ZW, Yang Z, Jiang CJ, Wang XZ, et al. In planta genetic transformation to produce CRISPRed high-oleic peanut. Plant Growth Regul. 2023;101:443–51.
86. Neelakandan AK, Wright DA, Traore SM, Chen X, Spalding MH, He G. CRISPR/Cas9 based site-specific modification of FAD2 cis-regulatory motifs in peanut (Arachis hypogaea L). Front Genet. 2022;13:849961.
87. Yuan M, Zhu J, Gong L, He L, Lee C, Han S, et al. Mutagenesis of FAD2 genes in peanut with CRISPR/Cas9 based gene editing. BMC Biotechnol. 2019;19:24.

Publisher's Note